

Oscillator Circuits For RTD Temperature Sensors

Author: Ezana Haile and Jim Lepkowski
Microchip Technology Inc.

INTRODUCTION

This application note shows how to design a temperature sensor oscillator circuit using Microchip's low-cost MCP6001 operational amplifier (op amp) and the MCP6541 comparator. Oscillator circuits can be used to provide an accurate temperature measurement with a Resistive Temperature Detector (RTD) sensor. Oscillators provide a frequency output that is proportional to temperature and are easily integrated into a microcontroller system.

RC oscillators offer several advantages in precision sensing applications. Oscillators do not require an Analog-to-Digital Converter (ADC). The accuracy of the frequency measurement is directly related to the quality of the microcontroller's clock signal and high-frequency oscillators are available with accuracies of better than 10 ppm.

RTDs serve as the standard for precision temperature measurements because of their excellent repeatability and stability characteristics. A RTD can be characterized over its temperature measurement range to obtain a table of coefficients that can be added to the measured temperature in order to obtain an accuracy better than 0.05°C. In addition, RTDs have a very fast thermal response time.

Two oscillator circuits are shown in Figures 1 and 2 that can be used with RTDs. The circuit shown in Figure 1 is a state variable RC oscillator that provides an output frequency that is proportional to the square root of the product of two temperature-sensing resistors. The circuit shown in Figure 2, which is referred to as an astable multi-vibrator or relaxation oscillator, provides a square wave output with a single comparator. The state variable oscillator is a good circuit for precision applications, while the relaxation oscillator is a good alternative for cost-sensitive applications.

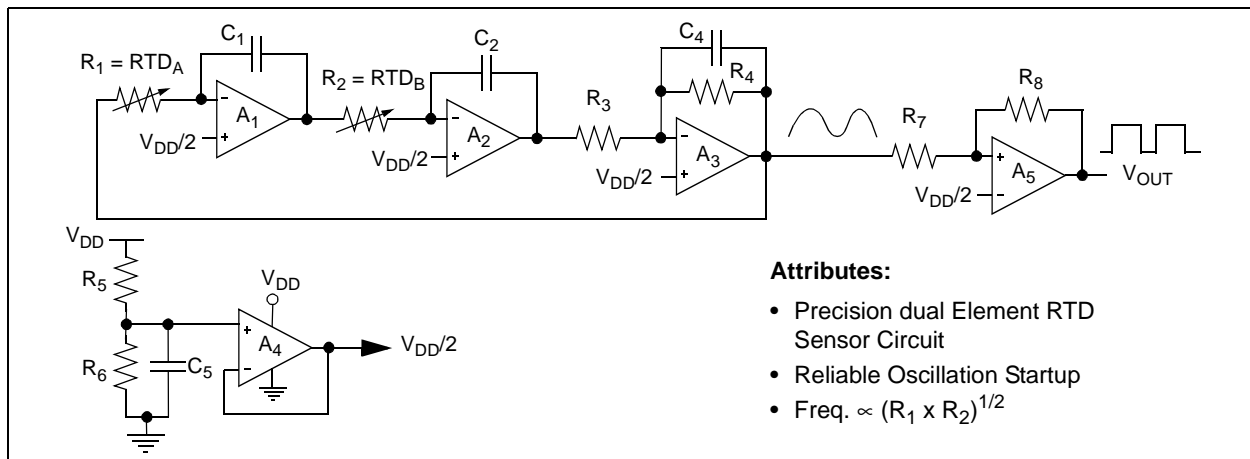


FIGURE 1: State Variable Oscillator.

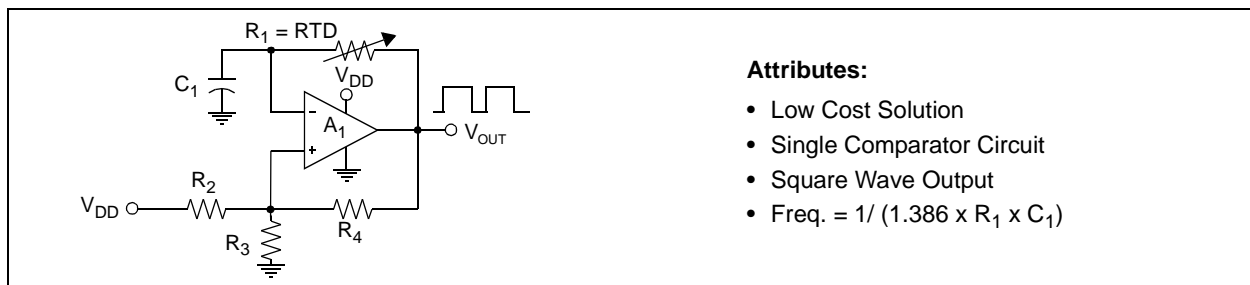


FIGURE 2: Relaxation Oscillator.

WHY USE A RTD?

RTDs are based on the principle that the resistance of a metal changes with temperature. RTDs are available in two basic designs: wire wound and thin film. Wire wound RTDs are built by winding the sensing wire around a core to form a coil, while thin film RTDs are manufactured by depositing a very thin layer of platinum on a ceramic substrate.

Table 1 provides a comparison of the attributes of RTDs, thermocouples, thermistors and silicon IC sensors. RTDs are the standard sensor chosen for precision sensing applications because of their excellent repeatability and stability characteristics. Also, RTDs can be calibrated to an accuracy that is only limited by the accuracy of the reference temperature.

TABLE 1: ATTRIBUTES OF RTDS, THERMOCOUPLES, THERMISTORS AND SILICON IC SENSORS

Attribute	RTD	Thermocouple	Thermistor	Silicon IC
Temperature Range	-200 to 850°C	-184 to 1260°C	-55 to +150°C	-55 to +125°C
Temperature (t) Accuracy	Class B = $\pm[0.012 + (0.0019 t) - 6 \times 10^{-7} t^2]$	Greater of $\pm 2.2^\circ\text{C}$ or $\pm 0.75\%$	Various, ± 0.5 to 5°C	Various, ± 0.5 to 3°C
Output Signal	$\approx 0.00385 \Omega/\Omega/^\circ\text{C}$	Voltage ($40 \mu\text{V}/^\circ\text{C}$)	$\approx 4\% \Delta R/\Delta t$ for $0^\circ\text{C} \leq t \leq 70^\circ\text{C}$	Analog, Serial, Logic, Duty Cycle
Linearity	Excellent	Fair	Poor	Good
Precision	Excellent	Fair	Poor	Fair
Durability	Good, Wire wound prone to open-circuit vibration failures	Good at lower temps., poor at high temps., open-circuit vibration failures	Good, Power Specification is derated with temperature	Excellent
Thermal Response Time	Fast (function of probe material)	Fast (function of probe material)	Moderate	Slow
Cost	Wire wound - High, Thin film - Moderate	Low	Low	Moderate
Package Options	Many	Many	Many	Limited, IC packages
Interface Issues	Small $\Delta R/\Delta t$	Cold junction compensation, Small ΔV	Non-linear resistance	Sensor is located on PCB

WHY USE AN OSCILLATOR?

There are several different circuit methods available to accurately measure the resistance of a RTD sensor. Figure 3 provides simplified block diagrams of three common RTD-sensing circuits. A constant current, voltage divider or oscillator circuit can be used to provide an accurate temperature measurement.

The constant current circuit uses a current source to create a voltage that is sensed with an ADC. A constant current circuit offers the advantage that the accuracy of the amplifier is not affected by the resistance of the wires that connect to the sensor. This circuit is especially useful with a small resistance sensor, such as an RTD with a nominal resistance of 100Ω , where the resistance of the sensor leads can be significant in proportion to the sensor's resistance. In remote sensing applications, the sensor is connected to the circuit via a long wire and multiple connectors. Thus, the connection resistance can be significant. The resistance of 18 gauge copper wire is $6.5 \text{ m}\Omega/\text{ft}$. at 25°C . Therefore, the wire resistance can typically be neglected in most applications.

The constant current approach is often used in laboratory-grade precision equipment with a 4-lead RTD. The 4-lead RTD circuits can be used to provide a Kelvin resistance measurement that nulls out the resistance of the sensor leads. Kelvin circuits are relatively complex and are typically used in only very precise applications that require a measurement accuracy of better than 0.1°C .

Another advantage of the constant current approach is that the voltage output is linear. While linearity is important in analog systems, it is not usually a critical parameter in a digital system. A table look-up method that provides linear interpolation of temperature steps of 5°C is adequate for most applications and can be easily implemented with a microcontroller.

The voltage divider circuit uses a constant voltage to create a voltage that is proportional to the RTD's resistance. This method is simple to implement and also offers the advantage that precision IC voltage references are readily available. The main disadvantage of both the voltage divider and constant current approach is that an ADC is required. The

accuracy of the voltage-to-temperature conversion is limited by the resolution of the ADC and the noise level on the PCB.

Oscillators offer several advantages over the constant current and voltage RTD sensing circuits. The main advantage of the oscillator is that an ADC is not required. Another key attribute of oscillators is that these circuits can produce an accuracy and resolution that is much better than an analog output voltage circuit. The accuracy of the frequency-to-temperature conversion is limited only by the accuracy of the counter or microcontroller time processing unit's high

frequency clock signal. High frequency clock signals are available with an accuracy better than 10 ppm over an operating temperature range of -40°C to $+125^{\circ}\text{C}$. In addition, the temperature sensitivity of the reference clock signal can usually be compensated with a simple calibration procedure.

Designers are often reluctant to use oscillators due to their lack of familiarity with these circuits. A negative feature with oscillators is that they can be difficult to troubleshoot and may not oscillate under all conditions. However, the state variable and relaxation oscillators provide very robust start-up oscillation characteristics.

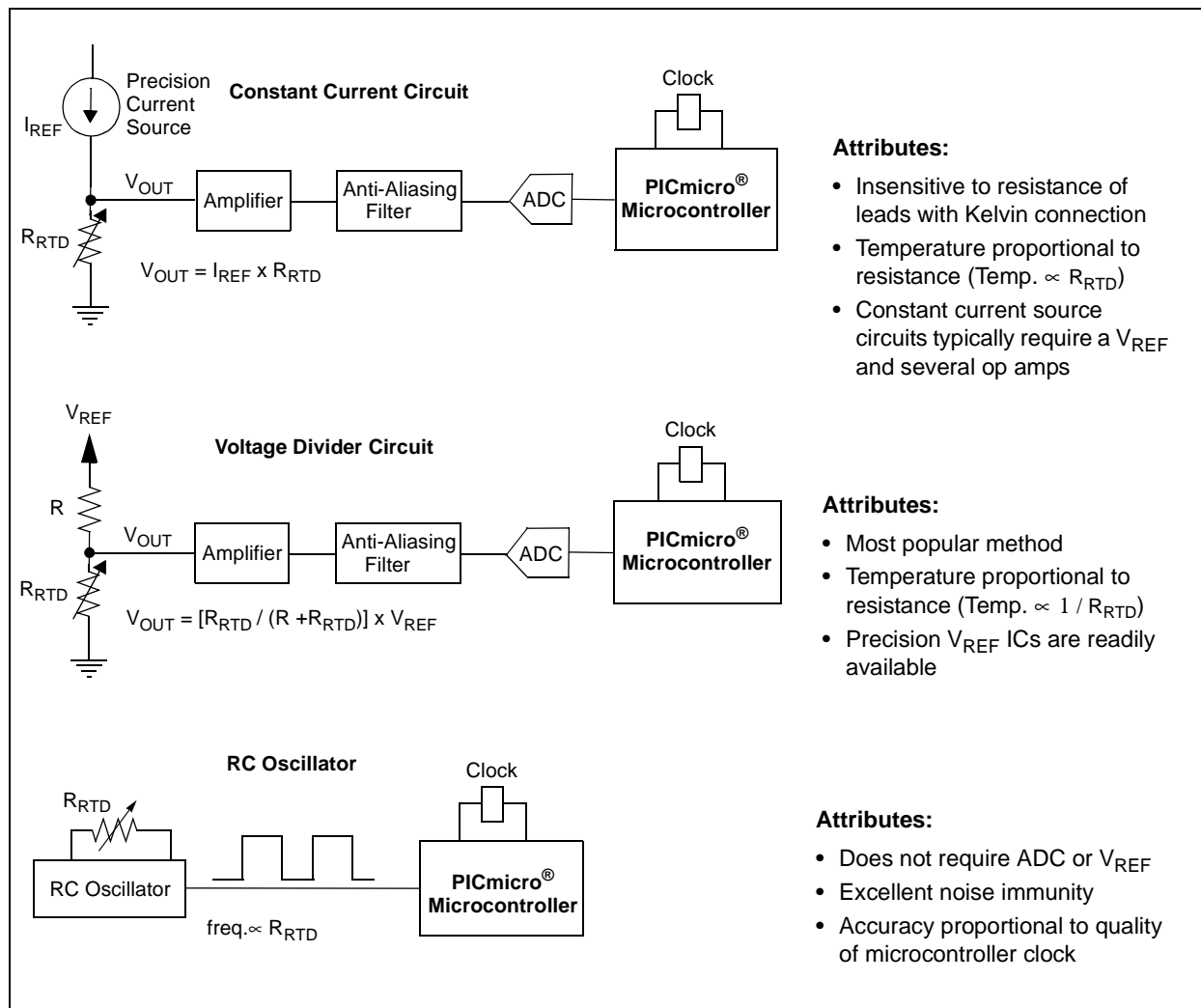


FIGURE 3: Common RTD Sensor Signal Conditioning Circuits.

STATE VARIABLE OSCILLATOR

Circuit Description

The schematic of the circuit is shown in Figure 1. The state variable oscillator consists of two integrators and an inverter. Each integrator provides a phase shift of 90°, while the inverter adds an additional 180° phase shift. The total phase shift of the three amplifiers is equal to 360°, with an oscillation produced when the output of the third amplifier is connected to the first amplifier.

The first integrator stage consists of amplifier A₁, RTD resistor R₁ (RTD_A) and capacitor C₁. The second integrator consists of amplifier A₂, RTD resistor R₂ (RTD_B) and capacitor C₂. For a dual RTD sensing application, R₁ ≅ R₂ and C₁ and C₂ should be the same value. The inverter stage consists of amplifier A₃, resistors R₃ and R₄ and capacitor C₄. The addition of capacitor C₄ helps ensure oscillation start-up.

A dual-element RTD is used to increase the difference in the oscillation frequency from the minimum to the maximum sensed temperature. The state variable oscillator's frequency is proportional to the square root of the product of the two RTD resistors (frequency ∝ (R₁ × R₂)^{1/2}). In contrast, a single-element RTD will produce a frequency output that is proportional to the square root of the RTD (frequency ∝ (R₁)^{1/2}). If the RTD resistance changes by a factor of two over the temperature sensing range, a dual-element sensor will provide an output that doubles in frequency. A single-element RTD will produce an output that varies by only 41% (i.e., √2).

The state variable circuit offers the advantage that a limit circuit is not required if rail-to-rail input/output (RRIO) amplifiers are used and the gain of the inverter stage A₃ is equal to one (i.e., R₃ = R₄). In contrast, most oscillators require a limit or clamping circuit to prevent the amplifiers from saturating. The gain of the integrator stages A₁ and A₂ is equal to one at the oscillation frequency, as shown by the detailed design equations provided in **Appendix B: "Derivation of Oscillation Equations"**.

Amplifier A₄ is used to provide the mid-supply reference voltage (V_{DD}/2) required for the single-supply voltage circuit. Resistors R₅ and R₆ form a voltage divider, while capacitor C₅ is used to provide noise filtering.

Comparator A₅ is used to convert the sinewave output to a square wave digital signal. The comparator functions as a zero-crossing detector and the switching point is equal to the mid-supply voltage (i.e., V_{DD}/2). Resistor R₈ is used to provide additional hysteresis (V_{HYS}) to the comparator.

Design Procedure

A simplified design procedure for selecting the resistors and capacitors is provided below. A detailed derivation of the equations is provided in **Appendix B: "Derivation of Oscillation Equations"**.

The state variable oscillator design equations can be simplified by selecting identical integrator stages (A₁ and A₂) and by using an inverter (A₃ with a gain of one). The identical integrator stages are implemented by using a dual-element RTD sensor and selecting C₁ = C₂. A unity-gain inverter stage is achieved if R₃ = R₄.

Simplified Equations:

Assume:

1. R₁ = R₂ = R (RTD_A = RTD_B)
2. C₁ = C₂ = C
3. R₃ = R₄

Design Procedure:

1. Select a desired nominal oscillation frequency for the RTD oscillator. Guidelines for selecting the oscillation frequency are provided in the **"System Integration"** section of this document.
2. C = 1/(2πR₀f₀).
where: R₀ = RTD resistance at 0°C
3. Select an op amp with a GBWP ≥ 100 × f_{max}.
where: f_{max} = 1 / (2πR_{min}C) and R_{min} = RTD resistance at coldest sensing temperature.
4. Select R₃ = R₄ equal to 1 to 10 times R₀.
5. Select C₄ using the following equations:
f_{-3dB} = 1 / (2πR₄C₄)
C₄ ≈ 1 / (2πR₄f_{-3dB})
where: f_{-3dB} ≅ op amp's GBWP

Listed below is the hysteresis equation for comparator A₅. The comparator functions as a zero-crossing detector that is offset by the voltage V_{DD}/2.

$$V_{HYS} = \frac{R_7}{R_7 + R_8} \times (V_{OUT(max)} - V_{OUT(min)})$$

$$V_{HYS} \cong \frac{R_7}{R_8} \times V_{DD} \quad \text{if } R_8 \gg R_7$$

State Variable Test Results

The components used in the evaluation design are listed in Table 2. The circuit was tested with lab stock components. The specifications of the 100 nF capacitors are not as good as the NPO porcelain ceramic capacitors used in the RSS error analysis shown in Table 4. The maximum capacitance available with the ATC700 series NPO capacitors is 5100 pF. The decrease in magnitude of C_1 and C_2 will increase the oscillation frequency from 21 kHz to 39 kHz for a RTD sensed temperature of -55°C to $+125^{\circ}\text{C}$. If smaller magnitude capacitors are used, a MCP6024 op amp with a GBWP of 10 MHz is recommended to minimize the op amp error on the accuracy of the higher oscillation frequency.

The test results are shown in Table 3 and Figure 4. The oscillation frequency was calculated using the measured values of R_1 , R_2 , R_3 , R_4 , C_1 and C_2 . The dual-element RTD sensors (R_1 and R_2) were tested by simulating a change in temperature with discrete resistors and measuring the resistance to a resolution of 100 m Ω . Capacitors C_1 and C_2 were measured to have a capacitance of 100.4 nF and 100.8 nF, respectively.

TABLE 2: STATE VARIABLE COMPONENTS

$R_1, R_2 =$	Dual Platinum Thin-Film RTD Temperature Sensor Omega 2PT1000FR1345 $R_0 = 1000\Omega$ Accuracy = Class B
$R_3, R_4, R_5, R_6, R_7 =$	1 k Ω
$R_8 =$	1 M Ω
$C_1, C_2 =$	100 nF
$C_4 =$	20 pF
$C_5 =$	1 μF
$V_{DD} =$ $V_{SS} =$	5.0V Ground
$A_1, A_2, A_3, A_4 =$	MCP6004 op amp (quad RRIO, GBWP = 1 MHz)
$A_5 =$	MCP6541 Push-Pull Output Comparator

TABLE 3: STATE VARIABLE OSCILLATOR TEST RESULTS

Simulated Temperature ($^{\circ}\text{C}$)	Resistor Values ($R_1 = R_2 =$)(Ω)	Calculated Frequency (Hz)	Measured Frequency (Hz)	Error (%)	Error ($^{\circ}\text{C}$)
-50.4	806	1961	1957	+0.20	0.52
-20.8	920	1718	1715	+0.16	0.42
0	1000	1581	1577	+0.24	0.62
26.0	1100	1440	1443	-0.23	0.60
51.9	1200	1317	1321	-0.29	0.75
75.3	1290	1225	1223	+0.24	0.62
98.7	1380	1146	1144	+0.20	0.52
122.1	1470	1076	1073	+0.25	0.65

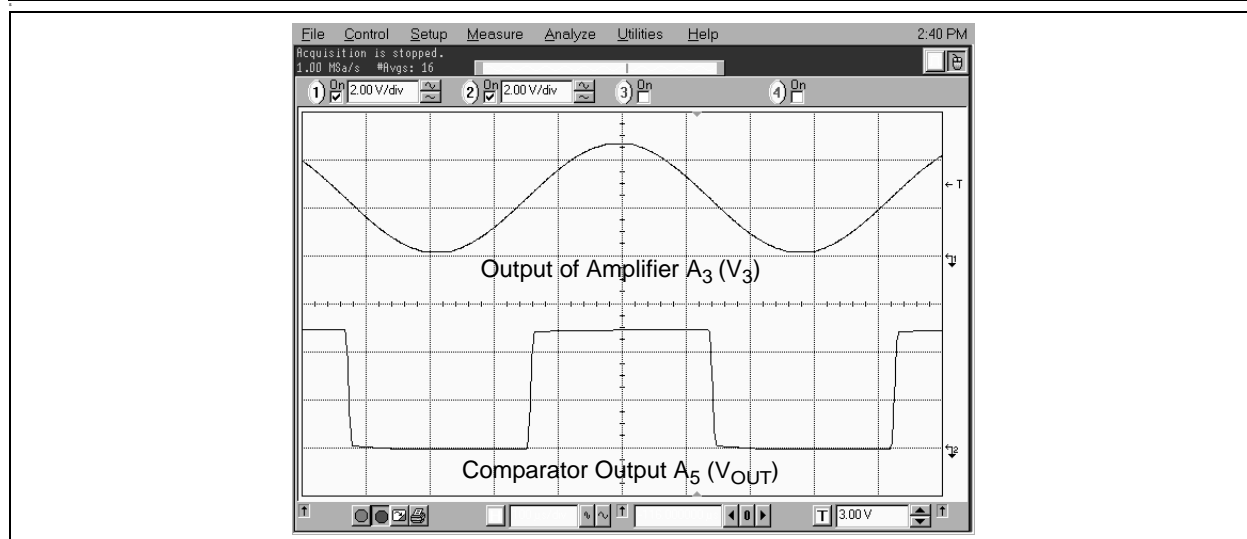


FIGURE 4: State Variable Oscillator Test Results ($R_1 = R_2 = 1000\Omega$).

Error Analysis

Error analysis is useful to predict the manufacturing variability, temperature stability and the drift in accuracy over time. The majority of the error, or uncertainty in the state variable oscillation frequency, results from the resistors and capacitors. The errors caused by the PCB layout and op amp are small in comparison. The frequency errors that result from the PCB layout can be minimized by using good analog PCB layout techniques. The error of the amplifier is minimized by selecting an op amp with a GBWP of approximately 100 times larger than the oscillator frequency.

Table 4 provides a Root Sum Squared (RSS) estimation of the resistor and capacitor errors on the frequency output of the state variable oscillator. Note that capacitor C_4 is not included in the table because it will not be a factor in the oscillation equation, if its magnitude is relatively small. The equation that specifies the accuracy of a class B RTD is given in **Appendix A: "RTD Selection"**. The RTD has a temperature accuracy of $\pm 0.15^\circ\text{C}$ at room temperature and $\pm 0.35^\circ\text{C}$ at $+125^\circ\text{C}$. Together, the state variable oscillator and a class B dual-element RTD will provide a temperature measurement accuracy of approximately $\pm 0.67^\circ\text{C}$ at room temperature and $\pm 1.07^\circ\text{C}$ at $+125^\circ\text{C}$.

Temperature compensation can be used to improve the accuracy of the circuit. The component tolerance error term of resistors R_3 and R_4 , capacitors C_1 and C_2 and the RTD resistors R_1 and R_2 can be minimized by calibrating the oscillator to a single known temperature. The magnitude of the resistor and capacitor temperature coefficient terms can be minimized by selecting low temperature coefficient components and by calibrating the circuit at multiple temperatures. Resistors with small temperature coefficients are readily available. However, the temperature coefficient of a capacitor is relatively large in comparison. A constant change in the capacitance can easily be compensated, though the temperature coefficient of a capacitor is usually not linear. The temperature coefficient of most capacitors is small at $+25^\circ\text{C}$ and much larger at the extreme cold and hot ends of the temperature range.

The aging or long-term stability error of the circuit is minimized by selecting components with a small drift rate. This term can also be reduced by using a burn-in procedure. Temperature compensation and burn-in options are discussed in the **"Oscillator Component Selection Guidelines"** section of this document. The state variable circuit and a class B RTD can be used to provide a measurement accuracy better than $\pm 0.1^\circ\text{C}$ with temperature compensation and a burn-in procedure.

TABLE 4: ERROR ANALYSIS OF RESISTORS, CAPACITORS AND RTD ON OUTPUT OF STATE VARIABLE OSCILLATOR (NOTE 4)

Error Term	Item	Sensitivity (Notes 1, 2 and 5)	Error @ $+25^\circ\text{C}$	Error @ $+125^\circ\text{C}$	Comments
Resistor Tolerance	R_3, R_4	-0.5, +0.5	100 ppm	100 ppm	Tolerance = 0.01% RNC90
Resistor TC	R_3, R_4	-0.5, +0.5	0 ppm	200 ppm	TC = 2 ppm/ $^\circ\text{C}$
Resistor Aging	R_3, R_4	-0.5, +0.5	50 ppm	50 ppm	ΔR at 2000 hours, 0.3W and $+125^\circ\text{C}$
Capacitor Tolerance	C_1, C_2	-0.5, -0.5	2500 ppm	2500 ppm	Tolerance = 0.25% NPO Porcelain Ceramic (ATC700B series, American Technical Ceramic)
Capacitor TC	C_1, C_2	-0.5, -0.5	0 ppm	3000 ppm	TC = 30 ppm/ $^\circ\text{C}$
Capacitor Aging	C_1, C_2	-0.5, -0.5	0 ppm (zero aging effect)	0 ppm (zero aging effect)	ΔC at 2000 hours, 200% WVDC and $+125^\circ\text{C}$
Capacitor Retrace	C_1, C_2	-0.5, -0.5	200 ppm	200 ppm	ΔC temperature hysteresis
RTD Accuracy	R_1, R_2	-0.5, -0.5	643 ppm	1340 ppm	Class B dual element RTD

Note 1: The sensitivity of the resistors is defined as the relative change in the oscillation frequency per the relative change in resistance ($(\Delta f_o/f_o)/(\Delta R/R)$).

2: The sensitivity of the capacitors is defined as the relative change in the oscillation frequency per the relative change in capacitance ($(\Delta f_o/f_o)/(\Delta C/C)$).

3: The temperature accuracy error (Δt) was calculated using the equations provided in Table 7.

4: ppm is defined as parts-per-million (i.e., 200 ppm = 0.02%).

5: The sensitivity equations are defined in **Appendix C: "Error Analysis"**.

TABLE 4: ERROR ANALYSIS OF RESISTORS, CAPACITORS AND RTD ON OUTPUT OF STATE VARIABLE OSCILLATOR (NOTE 4) (CON'T)

Error Term	Item	Sensitivity (Notes 1, 2 and 5)	Error @ +25°C	Error @ +125°C	Comments
Worst-Case Error Δfreq. (Δf) Δtemp. (Δt)			3493 ppm / 0.349% Δt = ±0.91°C	7390 ppm / 0.739% Δt = ±1.93°C	Note 3
RSS Error Δfreq. (Δf) Δtemp. (Δt)			2592 ppm / 0.259% Δt = ±0.67°C	4140 ppm / 0.414% Δt = ±1.07°C	Note 3

- Note 1:** The sensitivity of the resistors is defined as the relative change in the oscillation frequency per the relative change in resistance $((\Delta f_o/f_o)/(\Delta R/R))$.
- 2:** The sensitivity of the capacitors is defined as the relative change in the oscillation frequency per the relative change in capacitance $((\Delta f_o/f_o)/(\Delta C/C))$.
- 3:** The temperature accuracy error (Δt) was calculated using the equations provided in Table 7.
- 4:** ppm is defined as parts-per-million (i.e., 200 ppm = 0.02%).
- 5:** The sensitivity equations are defined in **Appendix C: "Error Analysis"**.

RELAXATION OSCILLATOR

Circuit Description

The relaxation oscillator shown in Figure 5 provides a resistive sensor oscillator circuit using the MCP6541 comparator. This circuit provides a relatively simple and inexpensive solution to interface a resistive sensor, such as a RTD to a microcontroller. This circuit topology requires a single comparator, a capacitor and a few resistors. The oscillator outputs a square wave with a frequency proportional to the change in the sensor resistance.

The analysis of this circuit begins by assuming that during power-up, the comparator output voltage is railed to the positive supply voltage (V_{DD}). Based on the values of R_2 , R_3 and R_4 , the voltage at V_{IN+} of the comparator can be determined. This voltage becomes a switching or trip voltage to toggle the output to V_{SS} as the voltage across the capacitor C_1 charges.

The comparator sources current to charge the capacitor through the feedback resistor (R_1). When the voltage across the capacitor rises above the voltage at V_{IN+} , the comparator drives the output down to the negative rail (V_{SS}). However, when the output voltage swings to V_{SS} , the trip voltage at V_{IN+} also changes. Now the comparator output stays at V_{SS} until the voltage across the capacitor discharges through R_1 . When the capacitor voltage falls below the voltage at V_{IN+} , the comparator drives the output up to the positive rail (V_{DD}). Therefore, the comparator swings the output voltage to the rails (V_{DD} and V_{SS}), every time the capacitor voltage passes the trip voltage. As a result, the comparator output generates a square wave oscillation.

Design Procedure

A simplified design procedure for selecting the resistors and capacitor C_1 is provided below. The relaxation oscillator design equations can be simplified by selecting the trip point voltages of the comparator circuit to be equal to $1/3 V_{DD}$ and $2/3 V_{DD}$ by using equal value resistors for R_2 , R_3 and R_4 . A detailed derivation of the oscillation equations and error terms is provided in **Appendix B: "Derivation of Oscillation Equations"**.

Simplified Equations:

Assume:

1. $R_1 = \text{RTD sensor}$
2. $R_2 = R_3 = R_4 = R$
3. $R \cong 10 \times R_0$

where: $R_0 = \text{RTD resistance at } 0^\circ\text{C}$

Design Procedure:

1. Select a desired nominal oscillation frequency for the RTD oscillator. Guidelines for selecting the oscillation frequency are provided in the **"System Integration"** of this document.
2. $C_1 = 1 / (1.386 R_0 f_0)$.
3. Select a comparator with an Output Short Circuit Current (I_{SC}) which is at least five times greater than the maximum output current to ensure start-up at cold and relatively good accuracy.

$$I_{OUT_MAX} = V_{DD} / R_{1_MIN}$$

$$I_{SC} = I_{OUT_MAX} / 5$$

where: $R_{1_MIN} = \text{RTD resistance at coldest sensing temperature and } V_{DD} \text{ is equal to the supply voltage.}$

Relaxation Oscillator Test Results

The oscillation frequency was calculated using fixed discrete resistors to simulate the RTD resistance, R_1 and the component values shown in Figure 5. A $0.68 \mu\text{F}$ tantalum capacitor was chosen for C_1 . The circuit uses the MCP6541 comparator.

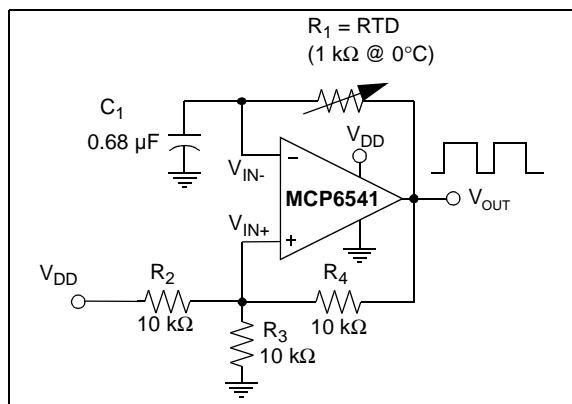


FIGURE 5: Relaxation Oscillator Component Values.

TABLE 5: RELAXATION OSCILLATOR TEST RESULTS

Simulated Temperature (°C)	RTD (Ω)	Calculated Frequency (Hz)	Measured Frequency (Hz)	Error (%)	Error (°C)
-51.7	801	1322.4	1303	-1.47	3.9
-18.2	930	1139.0	1124	-1.31	3.5
12.5	1048	1010.7	1000	-1.06	2.8
25.5	1098	964.7	955	-1.01	2.7
54.0	1208	876.9	867	-1.12	2.9
76.4	1294	818.6	811	-0.93	2.4
95.3	1367	774.9	769	-0.76	2.0
120.8	1465	723.0	717	-0.83	2.2

Table 5 shows a summary of the test results, while Figure 6 provides a picture of the oscillation frequency from the oscilloscope.

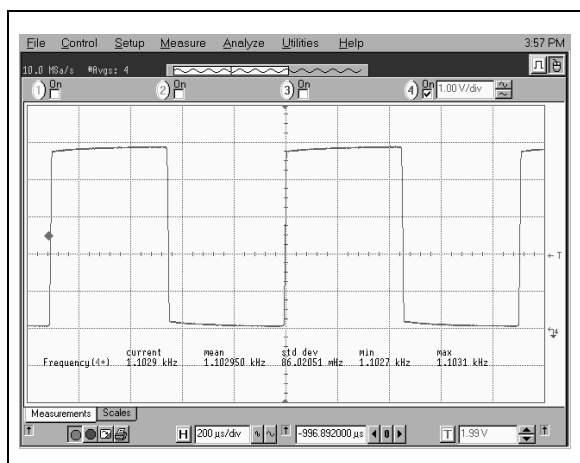


FIGURE 6: Measured Relaxation Oscillator Output.

A major error source in the relaxation oscillator is the comparator's output drive capability. When the output of the comparator toggles to V_{DD} or V_{SS} , the comparator has to source and sink the charge and discharge current. If the comparator output is current limited, it takes a longer period of time to charge and discharge the capacitor C_1 , which ultimately affects the oscillation frequency. The oscillation frequency needs to be properly selected so that the comparator's output limits introduce a relatively small error over the oscillation frequency range. This error source is described in **Appendix D: "Error Analysis of the Relaxation Oscillator's Comparator"**.

If a larger resistance RTD sensor is used, the comparator's output current is reduced and the accuracy of the circuit increases. RTD sensors are available in a number of nominal resistances, including 2000Ω and 5000Ω. The test results of Table 5 show that the relaxation oscillator's accuracy is greater at the larger resistances than at the smaller resistances. The 1000Ω RTD resistance was chosen because it is readily available in both wire wound and thin film

configurations. The growing popularity of the thin film technology has resulted in larger resistance RTDs at a reasonable cost.

Another factor that limits the accuracy of the relaxation oscillator is the relatively poor performance characteristics of the 0.68 μF capacitor. Recommendations on the selection of capacitor C_1 to maximize the accuracy of the oscillation frequency are provided in the section titled, "**Oscillator Component Selection Guidelines**".

Error Analysis

Table 6 provides a RSS estimation of the error of the resistors and capacitor on the output frequency of the relaxation oscillator. The test results from the previous section show that the comparator output drive capability limits the circuit accuracy. To minimize this affect, a smaller capacitor and larger RTD resistance can be used (see **Appendix D: "Error Analysis of the Relaxation Oscillator's Comparator"**).

The sensitivity equations for the relaxation oscillator are listed below. The sensitivity values of resistors R_3 and R_4 will be determined from the design equations provided in **Appendix B: "Derivation of Oscillation Equations"**. Note that R_2 does not have a sensitivity term because a change in the resistance changes the upper and lower trip voltages an equal amount at the inverting terminal and the voltage level difference between the trip voltages will remain constant. Although resistor R_2 does not play a critical role in determining the oscillation frequency, it is recommended that the circuit use a high-quality resistor equal to R_3 and R_4 .

$$f_o = \frac{1}{(1.386)(R_1 C_1)}$$

$$S_{R_1}^{f_o} = S_{C_1}^{f_o} = -1 \quad S_{R_3}^{f_o} = -S_{R_4}^{f_o} = -0.716$$

The RSS analysis shows that the resistors, capacitors and RTD errors limit the accuracy of the oscillator to approximately 1.2% at room temperature and 1.5% at +125°C, which corresponds to a temperature

AN895

resolution of $\pm 3.3^{\circ}\text{C}$ and $\pm 3.9^{\circ}\text{C}$, respectively. The equations correlating the oscillator's frequency to the temperature are provided in the "System Integration" section of this document.

The major error term of the relaxation oscillator is due to the tolerance of the capacitor. Thus, a calibration of the capacitor's nominal value can improve the accuracy of the temperature measurement. Options for providing temperature compensation to improve the

accuracy of the circuit are discussed in the "Oscillator Component Selection Guidelines" section of this document.

TABLE 6: ERROR ANALYSIS OF RELAXATION RESISTORS, CAPACITORS AND RTD (NOTE 4)

Error Term	Item	Sensitivity (Notes 1, 2 and 5)	Error @ +25°C	Error @ +125°C	Comments
Resistor Tolerance	R ₃ , R ₄	-0.716, +0.716	1000 ppm	1000 ppm	Tolerance = 0.1%, RN55 metal film
Resistor TC	R ₃ , R ₄	-0.716, +0.716	0 ppm	5000 ppm	TC = 50 ppm/°C
Resistor Aging	R ₃ , R ₄	-0.716, +0.716	5000 ppm	5000 ppm	ΔR at 2000 hours, 0.3W and +125°C
Capacitor Tolerance	C ₁	-1	10000 ppm	10000 ppm	Tolerance = 1%, NPO multi-layer ceramic (Presidio Components Inc.®)
Capacitor TC	C ₁	-1	0 ppm	3000 ppm	TC = 30 ppm/°C
Capacitor Aging	C ₁	-1	0 ppm (zero aging effect)	0 ppm (zero aging effect)	ΔC at 2000 hours, 200% WVDC and +125°C
Capacitor Retrace	C ₁	-1	200 ppm	200 ppm	ΔC temperature hysteresis
RTD Accuracy	R ₁	-1	643 ppm	1340 ppm	Class B RTD
Worst-Case Error					Note 3
Δfreq. (Δf)			19435 ppm/1.94%	30292 ppm/3.03%	
Δtemp. (Δt)			Δt = ±5.2°C	Δt = ±8.1°C	
RSS Error					Note 3
Δfreq. (Δf)			12400 ppm/1.24%	14677 ppm/1.47%	
Δtemp. (Δt)			Δt = ±3.3°C	Δt = ±3.9°C	

Note 1: The sensitivity of the resistors is defined as the relative change in the oscillation frequency per the relative change in resistance $((\Delta f_o/f_o)/(\Delta R/R))$.

2: The sensitivity of the capacitors is defined as the relative change in the oscillation frequency per the relative change in capacitance $((\Delta f_o/f_o)/(\Delta C/C))$.

3: The temperature accuracy error (Δt) was calculated using the equations provided in Table 7.

4: ppm is defined as parts-per-million (i.e., 200 ppm = 0.02%).

5: The sensitivity equations are defined in **Appendix C: "Error Analysis"**.

OSCILLATOR COMPONENT SELECTION GUIDELINES

Calibration and Burn-In

An oscillator used in sensor applications must have a tight tolerance, a small temperature coefficient and a low drift rate. The op amps, resistors and capacitors must be chosen carefully so that the change in the oscillation frequency results primarily from the change in the resistance of the RTD sensor and not from changes in the values of the other components.

An application that requires an oscillator accuracy of better than approximately $\pm 1^\circ\text{C}$ may require a temperature calibration and/or burn-in procedure to achieve the desired accuracy. A temperature compensation algorithm can be easily implemented using the EEPROM non-volatile memory of a PICmicro[®] microcontroller to store temperature correction data in a look-up table. The temperature coefficients are obtained by calibrating the circuit over the operating temperature range and comparing the measured temperature against the actual temperature. A polynomial curve-fitting equation of the frequency versus temperature data can also be used to improve the accuracy of the oscillator. Since the compensation coefficients will be unique for each PCB, the cost of manufacturing will increase.

The drift error of the resistors and capacitors can be significantly reduced by using a burn-in or temperature-cycling procedure. The long-term stability of resistors and capacitors is typically specified by a life test of 2000 hours at the maximum rated power and ambient temperature. Burn-in procedures are successful in stabilizing the drift error because the majority of the change in magnitude of resistors and capacitors typically occurs in the first 500 hours and the component drift is relatively small for the remainder of the test. A temperature-cycling procedure that exposes the components to fast temperature transients from cold-to-hot and hot-to-cold can be used to reduce the mechanical stresses inherent in the devices and improve the long-term stability of the oscillator.

Op Amp Selection

The appropriate op amp to use for the state variable oscillator can be determined with a couple of general design guides. First, the Gain Bandwidth Product (GBWP) should be a factor of approximately 100 times higher than the maximum oscillation frequency. Next, the Full Power Bandwidth (f_P) should be at least 2 times greater than the maximum oscillation frequency. The MCP6001 amplifier has a GBWP = 1 MHz (typ.) and a f_P of approximately 30 kHz, with $V_{DD} = 5\text{V}$. An oscillator with a frequency of approximately 10 kHz can be implemented with the MCP6001 with enough design margin that the op amp errors can be neglected.

Comparator Selection

The accuracy of the relaxation oscillator can be improved by using a comparator rather than an op amp for the amplifier. A comparator offers several advantages over an op amp in a non-linear switching circuit, such as a square wave oscillator. An op amp is intended to operate as a linear amplifier, while the comparator is designed to function as a fast switch. The switching specifications, such as propagation delay and rise/fall time of a comparator, are typically much better than an op amp's specifications. Also, the switching characteristics of an op amp typically only consist of a slew rate specification.

The non-ideal characteristics of a comparator will produce an error in the expected oscillation frequency. The offset voltage (V_{OS}), input bias current (I_B), propagation delay, rise/fall time and output current limit have an effect on the oscillation frequency. The non-ideal characteristics of the MCP6541 comparator are analyzed in **Appendix D: "Error Analysis of the Relaxation Oscillator's Comparator"** and the resulting frequency error of the relaxation oscillation is estimated. The test results of the relaxation oscillator show that an accuracy of approximately $\pm 3^\circ\text{C}$ can be achieved using the MCP6541 using a 1000Ω RTD. The accuracy of the relaxation oscillator can be improved by using a higher-resistance RTD and a higher performance comparator. However, the trade-off will be that the comparator's current consumption will be much higher.

Resistor Selection

The errors of the resistors can be minimized by selecting precision components and will be much less than the error from the capacitors. Metal film and foil resistors are two types of precision resistors that can be used in an oscillator. Metal film resistors are available with a tolerance of 0.01%, TC of ± 10 to ± 25 ppm/ $^\circ\text{C}$ and a drift specification of approximately 0.1 to 0.5%. RNC90 metal foil resistors are available with a tolerance of 0.01%, temperature coefficient of ± 2 ppm/ $^\circ\text{C}$ and a drift specification of less than 50 ppm. Vendors, such as Vishay[®] Intertechnology, Inc., offer a number of precision resistors that have much better specifications than the RNC90. These devices, however, are relatively expensive.

The operating environment of a resistor also can induce a change in resistance. Though the change of the ambient temperature is usually unavoidable; however, the power rating of a resistor can be chosen to minimize any self-heating from the I^2R drop of the device. Other factors, such as humidity, voltage coefficient (ΔR versus voltage) and thermal EMF (due to the temperature difference between the leads and self-heating) are small and can be neglected by using quality components and standard low noise analog PCB layout procedures.

Capacitor Selection

Capacitors have relatively poor performance when compared with resistors and are usually the component that limits the accuracy of an oscillator. Furthermore, precision capacitors are available in only relatively small capacitances. The state variable circuit reference design requires two 100 nF capacitors, while the relaxation oscillator needs a 0.68 μF capacitor in order for both circuits to have a nominal frequency of approximately 1 kHz, with a 1 kHz RTD. A capacitor with a tight tolerance, low temperature coefficient and small drift rate is available only in a maximum capacitance of approximately 100 nF. The relatively poor specifications of a microfarad-range capacitor limits the accuracy of the relaxation oscillator to approximately 3°C, unless temperature compensation is provided.

The major environmental error term of a capacitor is due to temperature hysteresis and is specified as the retrace error. Precision sensors can use temperature compensation to correct for a change of capacitance with temperature. However, it is difficult to correct for hysteresis errors. The retrace error of the American Technical Ceramic's ATC700 capacitors recommended for the state variable oscillator is specified at $\pm 0.02\%$. Other capacitor environmental errors result from the piezoelectric effect (ΔC versus voltage and pressure), the quality factor (Q) and resistance of the terminals. These errors are relatively small and can be neglected. In a sensor application, the oscillation frequency is well below the capacitor's maximum rated frequency and the amplitude of the voltage is small compared to the maximum Working Voltage DC (WVDC) rating of the capacitor.

RF and microwave capacitors are a good source of precision capacitors for the state variable oscillator. The ATC700 series NPO porcelain and ceramic capacitors have a tolerance of 0.1 pF, a temperature coefficient of $0 \pm 30 \text{ ppm}/^\circ\text{C}$ and a drift rating of 0.00%. Note that the vendor's data sheet states that the NPO dielectric has no change in capacitance with aging. However, the military standard for the device specifies the aging error as less than 0.02%. The trade-off with the high-frequency ATC700 NPO capacitors is that they are relatively small in magnitude and are only available in a maximum capacitance of 5100 pF.

A multi-layer or stacked NPO ceramic is the recommended capacitor for the relaxation oscillator. Vendors (such as Presidio, etc.) offer multi-layer NPO capacitors in values that include microfarads. Multi-layer capacitors are available with a tolerance of 1%, a temperature coefficient of $0 \pm 30 \text{ ppm}/^\circ\text{C}$ and a zero drift rating. Other types of capacitors available in a range of approximately 1 μF include tantalum and metallized polypropylene film. Tantalum capacitors are available with a tolerance of 1%, a temperature coefficient of $0 \pm 1000 \text{ ppm}/^\circ\text{C}$ and a drift rating of $\pm 1\%$. Polypropylene capacitors are available with a tolerance of 1%, a temperature coefficient of $0 \pm 250 \text{ ppm}/^\circ\text{C}$ and

a drift rating of 0.5%. One additional problem with the polypropylene capacitors is that their maximum temperature is typically specified at +85 to +105°C and some of the devices will not withstand the heat of an automated PCB soldering system.

SYSTEM INTEGRATION

Oscillator to PICmicro® Microcontroller Interface

The op amp oscillator can be easily integrated with a PICmicro microcontroller to determine the frequency of the oscillation or temperature. The oscillator can be connected to the PICmicro microcontroller with a standard digital input pin. However, a Schmitt-triggered input is recommended to provide additional noise immunity. A critical component in the frequency measurement system is the microcontroller's clock signal. The accuracy of the frequency measurement is directly related to the accuracy of the clock signal.

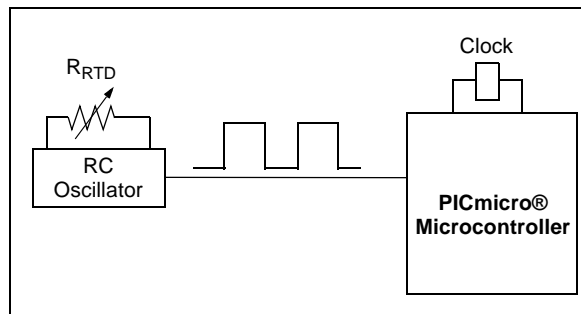


FIGURE 7: Typical RC Op Amp Oscillator Sensor System.

Microcontroller Clock

Typical microcontroller clock sources include crystal oscillators, crystals, crystal resonators, RC oscillators and internal microcontroller RC oscillators. Crystal oscillators are available with a temperature compensated accuracy better than 0.02%. They are also relatively expensive. Crystals with an accuracy of 0.1% are available at a moderate cost. Resonators typically have an accuracy of 0.5% and are relatively low in cost. The internal PICmicro microcontroller RC oscillators vary significantly (1%-50%) in accuracy and are not recommended for a frequency measurement application.

PICmicro Microcontroller Frequency Measurement Options

There are two different options available to measure oscillation frequency using a PICmicro microcontroller. One approach is to count the number of pulses in a fixed period of time, while the other is to count time between a fixed number of edges. Either one of these methods can be implemented for this application. It is important to note, however, the advantages and disadvantages of each solution.

The required resources for determining the frequency varies depending upon the processor bandwidth, available peripherals, and the resolution or accuracy desired. The fixed-time method could utilize a firmware delay or a hardware delay routine. While the firmware can poll for input edges, this consumes processor bandwidth. A more common implementation uses a hardware timer/counter to count the input cycles during a firmware delay. If a second timer is available, the delay can be generated using this timer, thus requiring minimal processor bandwidth. The fixed cycle method could utilize firmware to measure both time and poll input edges. However, this is processor-intensive and has accuracy limitations. A more common implementation is to utilize the Capture/Compare/PWM (CCP) module configured in Capture mode. This hardware uses the 16-bit TMR1 peripheral and has excellent accuracy and range.

FIXED TIME METHOD

The fixed time method consists of counting the number of pulses within a specific time window, such as 100 ms. The frequency is calculated by multiplying the count by the integer required to correlate the number of pulses in one second or the set time window.

When using a fixed time measurement approach, accuracy is relative to the input frequency versus measurement time. The measurement time is chosen by the designer based on the desired accuracy, input frequency and desired measurement rate. A faster measurement rate requires a shorter measurement window, thus reducing the resolution. A slower measurement rate allows a longer measurement

window and, therefore, increasing the resolution. For example, in this op amp oscillator application, the oscillator frequency is approximately 1 kHz at 0°C. If the measurement time is chosen to be 100 ms, there will be approximately 100 cycles within the fixed window. This provides an accuracy of approximately $\pm 0.5\%$. This measurement approach inherently minimizes the effect of error sources, such as the op amp oscillator's jitter, by simply averaging multiple edges prior to calculating the frequency.

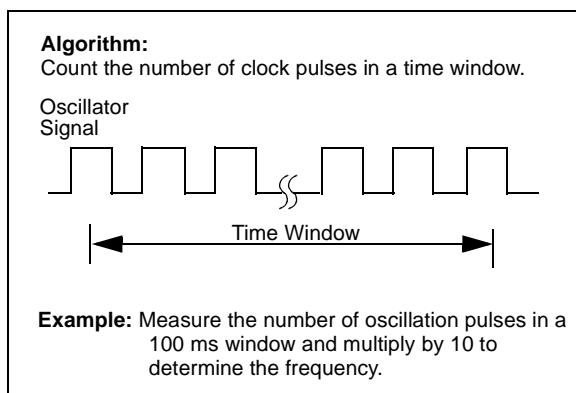


FIGURE 8: Fixed Time Method.

FIXED CYCLE METHOD

The fixed cycle approach is similar in concept to the fixed time approach. In the fixed cycle method, the number of cycles measured is fixed and the measurement time is variable. The concept is to measure the elapsed time for a fixed number of cycles. The number of cycles is chosen arbitrarily by the designer based on the desired accuracy, input frequency, desired measurement rate and PICmicro microcontroller clock frequency (F_{OSC}). The F_{OSC} determines the minimum time an edge can be resolved. The measurement error will be proportional to the total amount of time versus F_{OSC} . Increasing the number of cycles measured increases the total measurement time, thus reducing the error. Increasing F_{OSC} decreases the minimum time to resolve an edge, thus reducing the error. If the oscillator's nominal frequency is equal to 1 kHz and F_{OSC} is equal to 4 MHz, then the edge resolution is 1 μ s due to the microcontroller program counter incrementing once every four clock cycles ($F_{OSC}/4$). For an input frequency of 1 kHz, the measurement error becomes $1000 \pm 1 \mu$ s, or 0.1%. The error due to input signal jitter is significant only if few oscillation cycles are measured. Measuring more oscillation cycles inherently averages the input jitter at the expense of increasing the measurement time.

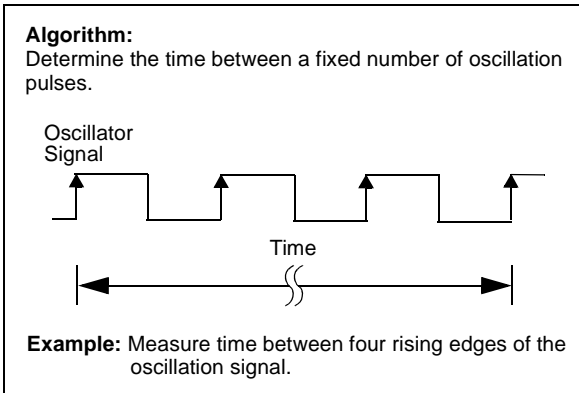


FIGURE 9: Fixed Cycle Method.

Oscillation Frequency versus Temperature

RTD oscillators provide a frequency output that is proportional to temperature. In this section, equations are provided that show the relationship between frequency and temperature. It should be noted that while resolution and accuracy are closely related, they are not identical. The accuracy of the RTD sensor,

oscillator circuit and the PICmicro microcontroller frequency measurement system has to be analyzed to determine the accuracy of the temperature measurement system.

RTDs have the characteristics that the change in resistance per temperature is very repeatable. If temperature correction is used with the RTD, the measurement accuracy of the system is limited only by the minimum resolution step size.

To illustrate the frequency-to-temperature relationship, let's assume that the state variable and relaxation oscillators are required to provide a temperature resolution of 0.25°C. The equations are developed using the resistance of the RTD at 0°C for convenience because R_0 is the standard value of resistance used to define a RTD. In addition, it is assumed that the change in the RTD's resistance is linear over the operating temperature range. A temperature change of 0.25°C will increase the resistance of the RTD by 0.9625Ω, which corresponds to a change of 0.096% in the oscillation frequency of both oscillators. The frequency-to-temperature relationship for the oscillators is shown in Table 7.

TABLE 7: FREQUENCY VERSUS TEMPERATURE FOR $\Delta t = 0.25^\circ\text{C}$

Term	Equation	
State Variable Oscillator		
ΔR	$R_0[1+\alpha(\Delta t)]-R_0$	$\cong 1000\Omega[1+(0.00385^\circ\text{C}^{-1})(0.25^\circ\text{C})] - 1000\Omega$ $\cong 0.9625\Omega$
$f_o @ t_o$	$[1 / (2\pi R_o C)]$	$= 1/(2 \pi (1000\Omega)(100 \text{ nF}))$ $= 1591.55 \text{ Hz } (P = 628.3 \mu\text{s})$
$f_o @ (t_o+\Delta t)$	$[1/(2\pi(R_o+\Delta R)C)]$	$= [1/(2\pi(1000 + 0.9625\Omega)(100 \text{ nF}))]$ $= 1590.02 \text{ Hz } (P = 628.9 \mu\text{s})$
Δf	$f_o(t_o)-f_o(t_o+\Delta t)$	$= 1.53 \text{ Hz } (0.096\%)$
Period (ΔP)	$P_o(t_o+\Delta t)-P_o(t_o)$	$= 628.9 - 628.3 \mu\text{s}$ $= 600 \text{ ns}$
Relaxation Oscillator		
ΔR	$R_0[1+\alpha(\Delta t)]-R_0$	$\cong 1000\Omega[1+(0.00385^\circ\text{C}^{-1})(0.25^\circ\text{C})] - 1000\Omega$ $\cong 0.9625\Omega$
$f_o @ t_o$	$[1/(2 \pi R_o C)]$	$= 1/[(1.386)(1000\Omega)(0.68 \mu\text{F})]$ $= 1061.8 \text{ Hz } (P = 941.8 \mu\text{s})$
$f_o @ (t_o+\Delta t)$	$[1 / (2 \pi (R_o+\Delta R)C)]$	$= 1/[(1.386)(1000+0.9625\Omega)(0.68 \mu\text{F})]$ $= 1060.7 \text{ Hz } (P = 942.7 \mu\text{s})$
Δf	$f_o @ t_o - f_o @ (t_o+\Delta t)$	$= 1.021 \text{ Hz } (0.096\%)$
Period (ΔP)	$P_o @ (t_o+\Delta t) - P_o @ t_o$	$= 942.7 - 941.8 \mu\text{s}$ $= 900 \text{ ns}$

Legend: $\Delta t = |t - t_o|$
 R_0 = RTD resistance at 0°C
 ΔR = change in resistance per Δt
 C = capacitance of C_1 and C_2
 $f_o @ t_o$ = oscillation frequency at 0°C
 Δf = change in oscillator frequency per ΔR
 ΔP = change in oscillator period per ΔR ($\Delta P = 1/\Delta f$)

Required Accuracy of the PICmicro Microcontroller Frequency Measurement

The accuracy of the PICmicro microcontroller time measurement method required to achieve a desired temperature resolution must also be analyzed. The accuracy of a microcontroller frequency measurement is directly related to the accuracy of the clock source. It is recommended that the PICmicro microcontroller's clock signal have an accuracy equal to, or 10 times better than, the accuracy of the oscillator. For a system that requires a resolution of 0.25°C ($\Delta f \cong 0.1\%$ or 1000 ppm), a PICmicro microcontroller clock signal with an accuracy of 10 to 100 ppm is required.

High accuracy oscillators are available; however, they are relatively expensive. The high accuracy oscillators usually include temperature compensation, with some devices having a micro-heater inside the oscillator that maintains a stable temperature for the crystal. An alternative to purchasing an expensive, high-accuracy clock signal is to use a software routine to implement temperature compensation. If the PICmicro microcontroller and oscillator are calibrated using a method such as a look-up table with correction coefficients, the tolerance and temperature coefficient of the clock signal can be corrected. Providing clock compensation will require individual calibration at the PCB that will be provided by forming a clock count versus temperature relationship.

The clock signal also has an error similar to the retrace error of a capacitor. This temperature hysteresis error can not be easily calibrated because the magnitude of the error is typically not repeatable and depends on the temperature history. Other oscillator errors such as the long term drift can be reduced with a burn-in or temperature cycling procedure.

Conclusion

RTD sensors have a very accurate resistance-to-temperature characteristic and are the standard temperature sensor for precision measurements. The main disadvantage of RTD sensors is that they are relatively expensive compared to other temperature sensors. The availability of thin film RTDs has lowered the price of these sensors, making RTDs economically feasible for many new applications. Another advantage of RTD sensors is that their thermal response time is very fast compared to other temperature sensors. For example, RTDs with a response time of a few milliseconds are used in hot wire anemometers to measure fluid flow.

Precision sensing oscillators can be created using CMOS op amps and comparators. CMOS ICs offer the advantages of a good bandwidth, low supply voltage and power consumption. However, their DC specifications are relatively modest compared to bipolar devices. Oscillators are relatively immune to DC specifications like input offset voltage (V_{OS}), making the MCP6001 and the MCP6541 CMOS op amp and comparator a good design choice for these precision sensing circuits.

The inexpensive MCP6001 op amp can be used to create an oscillator that can be used to accurately measure temperature. The state variable oscillator is a good circuit for precision applications, especially dual-element RTD sensors. The state variable oscillator and a class B dual element RTD can be used to provide a temperature measurement equal to $\pm 0.67^{\circ}\text{C}$ at room temperature and $\pm 1.07^{\circ}\text{C}$ at 125°C . Note that the accuracy of the measurement can be greatly improved by implementing one of the temperature compensation methods described in this document.

The relaxation oscillator offers a single comparator solution for cost-sensitive applications. It is a simple solution for an application that needs the fast thermal response time of RTD, with a temperature measurement accuracy approximately equal to $\pm 3^{\circ}\text{C}$.

Low cost and a simple interface circuit are terms that traditionally have not been associated with RTDs. Precision sensing oscillators can be created using Microchip's low-cost MCP6001 op amp and MCP6541 comparator. The main advantage of the oscillator circuits is that they do not require an ADC.

Acknowledgments

The authors appreciate the assistance of Jim Simons in creating the “**System Integration**” section.

References

- [1]. AN687, “Precision Temperature Sensing with RTD Circuits”, Baker, B., Microchip Technology Inc., 1999.
- [2]. “Time to Learn Your RTDs”, Gauthier, R., Sensors, May 2003.
- [3]. International Electrotechnical Commission (IEC), “Specification IEC 60751, Industrial Platinum Resistance Thermometer Sensors”, 1995 (amendment 2).
- [4]. “Resistance Temperature Detectors: Theory and Standards”, King, D., Sensors, October 1995.
- [5]. AN866, “Designing Operational Amplifier Oscillator Circuits for Sensor Applications”, Lepkowski, J., Microchip Technology Inc., 2003.
- [6]. “The ABCs of RTDs”, McGovern, Bill, Sensors, November 2003.
- [7]. “Introductory Systems Engineering”, Truxal, J., McGraw-Hill, N.Y., 1972.
- [8]. “Analog Filter Design”, Ch. 19, Op Amp Oscillators, Van Valkenburg, M., Saunders College Publishing, Fort Worth, 1992.

APPENDIX A: RTD SELECTION

Theory of Operation

RTDs are based on the principle that the resistance of a metal changes with temperature. A temperature sensor can be produced by building a precision resistor with a nominal resistance at a specific temperature (R_0), which typically is 0°C. The temperature measurement is then performed by comparing the resistance at the unknown temperature to the value at the calibration temperature. References [2], [3], [4] and [6] provide more details on RTDs.

RTD Options

RTDs are available in several different sensing metals, including platinum, nickel, copper and a nickel/iron alloy. Platinum is the most popular RTD metal used because of its superior stability, excellent linearity and wide temperature-sensing range. The resistive sensing element is available in two basic designs: wire wound and thin film. Wire wound RTDs are built by winding the sensing wire around a core to form a coil that is then covered with an insulation material. Thin film RTDs are manufactured by depositing a very thin layer of platinum on a ceramic substrate which is coated with either epoxy or glass to provide strain relief for the external lead wires and to protect the metal from the environment.

Wire wound RTDs have been available for a number of years and the large volume of manufacturing experience produces a sensor with very precise and repeatable temperature specifications. The advantages of wire wound RTDs include a wide temperature-sensing range, high-power rating, excellent repeatability and superior stability. The disadvantages of wire wounds are that they are expensive, available in a limited number of package options and are relatively fragile.

Thin film RTDs are a relatively new sensing technology that has been driven by advances in IC process fabrication techniques. The main advantage of thin film RTDs is that they are relatively inexpensive compared to wire wound RTDs. Thin film RTDs are cheaper to build because the platinum sensing element is typically just 10 to 100Å thick, which also allows for a higher resistance value and a wide range of package options. The main disadvantage of thin film RTDs is that they are not as accurate, or as stable, as wire wound sensors.

Accuracy Specifications

In order to establish the advantages of a RTD, it is necessary to define the temperature measurement terms of accuracy, precision, repeatability and stability. The accuracy of a temperature sensor is defined as how close the detected temperature matches the true temperature. In other words, accuracy defines how closely the resistance of the RTD follows the tabulated resistance tables that serve as the standard. In contrast, precision relates to how close the RTD's resistance is to a group of other RTD sensors. Precision is an important factor in determining the interchangeability of a sensor and the ability of the sensor to measure a small temperature gradient. Repeatability is defined as the sensor's ability to reproduce its previous measurement values. Though stability is similar to repeatability, stability is typically defined as the long-term drift of the sensor over a period of time.

A RTD's repeatability specification is the parameter that establishes this sensor as the standard for high-accuracy temperature measurements. A RTD can be characterized against temperature to obtain a table of temperature correction coefficients and the correction can be added to the temperature recording to provide a measurement accuracy of greater than 0.05°C. The repeatability error of an RTD is typically considered to be so small that it is essentially unmeasurable, while a rating for the long-term stability is usually less than 0.05°C/yr.

The temperature accuracy for a Class B RTD per the IEC 751 specification is listed below:

$$t = \pm[0.12 + (0.0019|t|) - (6 \times 10^{-7} t^2)]$$

t = Temperature Accuracy

The accuracy of a class B sensor is adequate for most applications and the higher accuracy class. A specification is typically used only in laboratory-grade temperature instrumentation. Figure 10 provides a graph of the temperature accuracy of a Class B RTD.

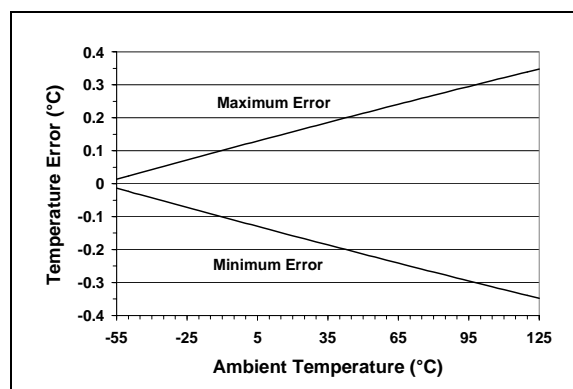


FIGURE 10: Accuracy of a Class B RTD.

Resistance versus Temperature

The International Electrotechnical Commission (IEC) has established the IEC-60751 standard for the resistance-to-temperature specifications of a RTD (Reference [3]). This standard produces a sensor that is interchangeable because the resistance to temperature relationship is identical for a class A or B sensor produced by any manufacturer.

A first order linear equation can be used to describe the RTD's resistance for a temperature between 0°C and 100°C. This equation is modeled by the temperature coefficient or alpha (α), which defines the average change in resistance per unit temperature change from the freezing point (0°C) to the boiling point of water (100°C). Note that the alpha standard is specific to a 100 Ω RTD at 0°C. However, this alpha is widely accepted as the standard temperature coefficient of commercially available RTDs that range from a nominal resistance at 0°C of 100 Ω to 10,000 Ω .

The linear first order equation is shown below:

$$R_t = R_o [1 + \alpha(t-t_o)] \text{ for } 0^\circ\text{C} \leq t \leq 100^\circ\text{C}$$

Where:

R_t = resistance at temperature t

R_o = resistance at calibration temperature t_o
(t_o typically is equal to 0°C)

t = temperature (°C)

α = temperature coefficient of resistance (°C⁻¹)
= 0.00385°C⁻¹

If the sensed temperature is less than 0°C or greater than 100°C, the RTD's resistance should be calculated using the Callendar-Van Dusen equation. The third order Callendar-Van Dusen equation is required to compensate for the slight non-linearity of the RTD over a wide temperature range. The operating range of a class B RTD is specified from -200°C to +850°C based on the IEC 751 specification.

The Callendar-Van Dusen equation is listed below:

$$R_t = R_o [1 + At + Bt^2] \text{ for } -200^\circ\text{C} \leq t < 0^\circ\text{C}$$

$$R_t = R_o [1 + At + Bt^2 + C(t-100)t^3]$$

for 0°C ≤ t ≤ 850°C

Where:

$A = 3.90830 \times 10^{-3}$ (°C⁻¹)

$B = -5.77500 \times 10^{-7}$ (°C⁻²)

$C = -4.18301 \times 10^{-12}$ (°C⁻⁴)

Comparisons of the RTD's resistance calculated using the first order and third order equations are shown in Figure 11 and Figure 12. The variance between the two equations is less than 0.1% (or approximately 0.2°C) for temperatures between -15°C and +120°C. The simpler linear first order equation can be used to calculate the resistance. However, the second order Callendar-Van Dusen equation should be used if the RTD is used to measure temperatures over a wider temperature range.

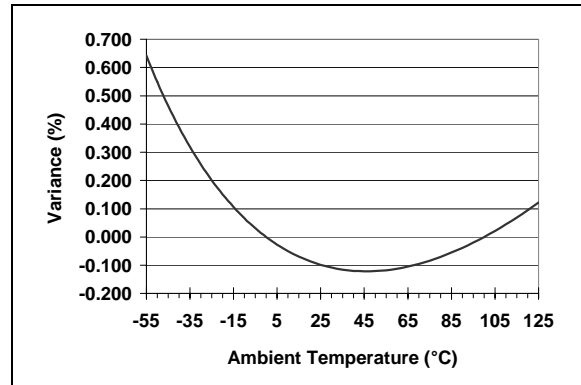


FIGURE 11: Percentage Variance between the First Order Linear and Third Order Polynomial Resistance vs. Temperature Characteristics for $-55 \leq t \leq +125^\circ\text{C}$.

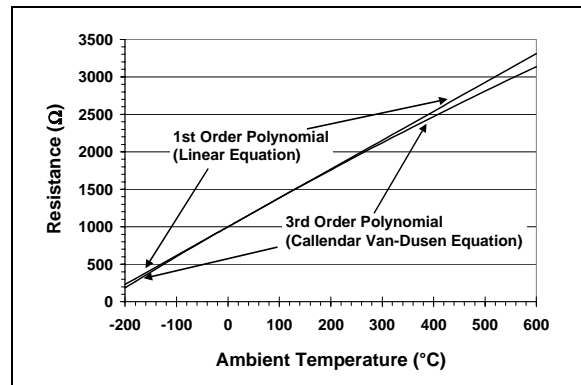


FIGURE 12: Resistance Variance between the First Order Linear and Third Order Polynomial Resistance versus Temperature Characteristics for $-200 \leq t \leq +600^\circ\text{C}$.

APPENDIX B: DERIVATION OF OSCILLATION EQUATIONS

OSCILLATOR THEORY

An oscillator is a positive feedback control system that generates a self-sustained output without requiring an input signal. Figure 13 provides a block diagram of an oscillator and the definition of the oscillation terms. Additional details on op amp oscillators are provided in references [7] and [8]. A procedure for deriving the oscillation design equations is provided in reference [5].

The oscillation frequency of an oscillator formed with multiple op amps (such as the state variable circuit) can be analyzed by finding the poles of the denominator of the transfer equation $T(s)$. Or equivalent to the zeroes of the numerator $N(s)$ of the characteristic equation (Δs) as shown in Figure 13.

In contrast, the design equations for the single comparator relaxation oscillator will be determined by analyzing the circuit as a comparator. The equations formed at the inverting and non-inverting terminals show that the output of the amplifier will swing from the V_{DD} to the V_{SS} power supply rails at a rate proportional to the charge and discharge time of the capacitor.

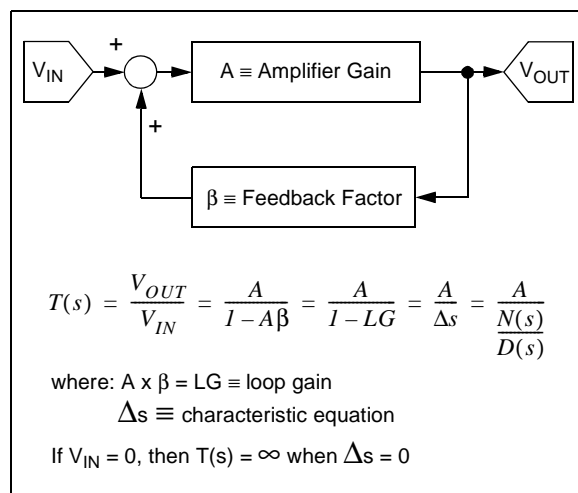


FIGURE 13: Oscillator Block Diagram.

STATE VARIABLE OSCILLATION EQUATIONS

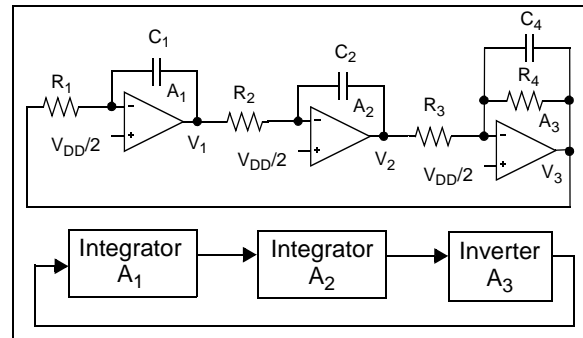


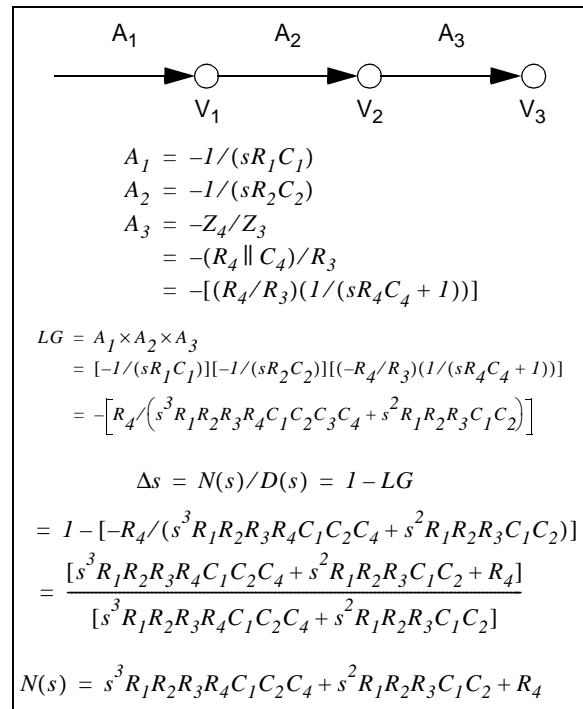
FIGURE 14: State Variable Oscillator.

STEP 1: FIND LG AND Δs

The oscillation frequency is determined by finding the poles of the denominator of the transfer equation $T(s)$. Or equivalent to the zeroes of the numerator $N(s)$ of the characteristic equation (Δs). Figure 14 provides a simplified schematic of the state variable oscillator. The first step in the procedure is to find the Δs equation by breaking the feedback loop and obtaining the gain equation at each op amp in order to calculate the loop gain (LG).

$$T(s) = \frac{A}{1 - LG} = \frac{A}{\Delta s} = \frac{A}{\frac{N(s)}{D(s)}}$$

The loop gain is found by breaking the oscillator loop, as shown below:



AN895

STEP 2: SOLVE $N(s) = 0$ AND FIND ω_0

An equation for the oscillation frequency ω_0 can be established by dividing the $N(s)$ term by $s^2 + \omega_0^2$ and solving the remainder to be equal to zero. Though this method is easy to use with third order systems, the algebra can be tedious with higher order systems. The division method is described in reference [7] and is based on factoring the characteristic equation to have an $s^2 + \omega_0^2$ term. The third order pole locations are at $s = \pm j\omega_0$ and $s = -b$ when the equation is factored in the form of $(s + b)(s^2 + \omega_0^2)$.

Routh's stability criterion provides an alternative method to analyze the $N(s)$ equation without the necessity of factoring the equation. References [5], [7] and [8] provide further information on the Routh method.

Note that C_4 does not appear in the oscillation equation. The gain of amplifier A_3 will not be a function of C_4 if the oscillation frequency is less than the cut-off frequency of the low pass filter formed by C_4 and R_4 .

Step 2:

$$N(s) = s^3 R_1 R_2 R_3 R_4 C_1 C_2 C_4 + s^2 R_1 R_2 R_3 C_1 C_2 + R_4$$

$$s^2 + \omega_0^2 \sqrt{\begin{array}{r} s R_1 R_2 R_3 R_4 C_1 C_2 C_4 + R_1 R_2 R_3 C_1 C_2 \\ \hline s^3 R_1 R_2 R_3 R_4 C_1 C_2 C_4 + s^2 R_1 R_2 R_3 C_1 C_2 + R_4 \\ -s^3 R_1 R_2 R_3 R_4 C_1 C_2 C_4 + \\ \hline s^2 R_1 R_2 R_3 C_1 C_2 + -s \omega_0^2 R_1 R_2 R_3 R_4 C_1 C_2 C_4 + R_4 \\ -s^2 R_1 R_2 R_3 C_1 C_2 + -\omega_0^2 R_1 R_2 R_3 C_1 C_2 \\ \hline -s \omega_0^2 R_1 R_2 R_3 R_4 C_1 C_2 C_4 + R_4 - \omega_0^2 R_1 R_2 R_3 C_1 C_2 \end{array}}$$

Set the s^0 remainder term equal to zero and solve for ω_0^2 .

$$R_4 - \omega_0^2 R_1 R_2 R_3 C_1 C_2 = 0$$

$$\omega_0 = \sqrt{\frac{R_4}{R_1 R_2 R_3 C_1 C_2}}$$

If:

1. $R_1 = R_2 = R$
2. $C_1 = C_2 = C$
3. $R_3 = R_4$

Then

$$\omega = (1/RC), \text{ period } (P) = 2\pi RC \\ \text{and } f = 1 / 2\pi RC$$

STEP 3: SUB-CIRCUIT DESIGN EQUATIONS

The third step analyzes the gain equation at each amplifier. Note that the gain of integrator stages will always be equal to one. As the RTD changes in resistance, the frequency will change in a proportional manner to maintain the gain of one.

Integrator A_1
Gain $A_1 = -1 / (2\pi f R_1 C_1)$

Integrator A_2
Gain $A_2 = -1 / (2\pi f R_2 C_2)$

Inverter A_3
Gain = $-[(R_4/R_3)(1/(sR_4C_4 + 1))]$

STEP 4: VERIFY $|LG| \geq 1$

The final step in the procedure verifies that the loop gain is equal to or greater than one, after the R and C component values have been chosen.

Assume:

1. $R_1 = R_2 = R$
2. $C_1 = C_2 = C$
3. $R_3 = R_4$

$$|A_1| = |A_2| = |A_3| = 1 \\ LG = |A_1 \times A_2 \times A_3| = 1$$

Relaxation Oscillator Design Equations

In this section, the equations that describe the circuit oscillation are derived. From these equations, the relationship of the oscillation frequency to the ambient temperature is quantified. Also, equations are developed for the error sources of the circuit.

The trip voltages at V_{IN+} can be determined using R_2 , R_3 and R_4 with respect to V_{DD} and V_{OUT} . The resistor network shown in Figure 2 can be simplified to the Thevenin Equivalent circuit for ease of calculation as shown in Figure 15. Initially, the Input Offset Voltage (V_{OS}) and the Input Bias Current (I_B) terms of the comparator will be ignored for simplification.

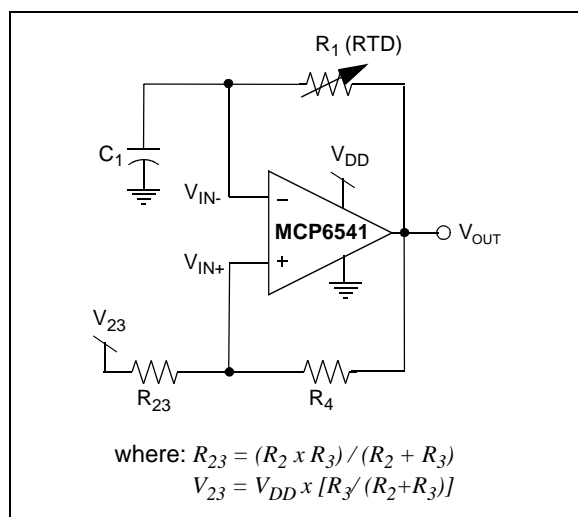


FIGURE 15: Thevenin Equivalent Circuit.

Realistically, the output stage of any push-pull output comparator does not exactly reach the supply rails, V_{DD} and V_{SS} . It approaches the rails to a point where the difference can be negligible. This is specified in the data sheet as high (V_{OH}) and low (V_{OL}) level output voltage. The MCP6541 comparator output voltage will be within 200 mV from the supply rails at 2 mA of source current. V_{OH} and V_{OL} increase as the comparator source or sink current increases (see Figure 17). Therefore, the capacitor C_1 and the trip voltages at the non-inverting input are driven by the V_{OH} and V_{OL} instead of V_{DD} and V_{SS} .

The trip voltage at V_{IN+} , which triggers the output to swing from V_{OH} to V_{OL} or from V_{OL} to V_{OH} , are referred to as V_{THL} and V_{TLH} , respectively. These trip voltages can be determined as follows using the Superposition Principle of circuit analysis.

$$V_{THL} = V_{OH} \left(\frac{R_{23}}{R_{23} + R_3} \right) + V_{23} \left(\frac{R_4}{R_{23} + R_4} \right)$$

$$V_{TLH} = V_{OL} \left(\frac{R_{23}}{R_{23} + R_3} \right) + V_{23} \left(\frac{R_4}{R_{23} + R_4} \right)$$

Using the equations below, the desired V_{THL} and V_{TLH} voltages can be set by properly selecting the corresponding resistors.

For example, if $R_2 = R_3 = R_4 = 10 \text{ k}\Omega$ and assuming that $V_{OH} = V_{DD}$ and $V_{OL} = V_{SS}$, then by substituting these values in the above equations, the trip voltages can be determined to be:

$$V_{THL} = 2/3 V_{DD}$$

$$V_{TLH} = 1/3 V_{DD}$$

Assuming that the sensor resistance is given at the test condition (for example, RTD resistance 1000Ω at 0°C), the oscillation frequency depends on the value of the capacitor C_1 . This frequency relates to the time that the capacitor charges and discharges through V_{OH} and V_{OL} .

The voltage across a capacitor changes exponentially, as shown below:

$$V_{CAP} = V_{final} + (V_{initial} - V_{final}) e^{-(t/\tau)}, t > 0$$

Where:

- τ = time constant defined by $R_1 \times C_1$
- t = time
- V_{CAP} = capacitor voltage at a given time t
- $V_{initial}$ = capacitor voltage at $t = 0$.
- V_{final} = capacitor voltage $t = \infty$

This equation describes the change in voltage across the capacitor with respect to time. This relationship can be used to calculate the oscillation frequency. Note that the capacitor charges and discharges up to the trip voltages V_{THL} and V_{TLH} , which are set by R_2 , R_3 and R_4 .

The following equation substitutes the variables in the above capacitor equation to solve for t and calculate the charging and discharging times.

When C_1 is charged through V_{OH} :

$$V_{THL} = V_{OH} + (V_{TLH} - V_{OH}) e^{-t_{charge}/\tau}$$

Solving for t :

$$t_{charge} = \tau \ln \left(\frac{V_{THL} - V_{OH}}{V_{TLH} - V_{OH}} \right)$$

Where:

t_{charge} = time for the capacitor to charge from V_{TLH} to V_{THL} .

AN895

When C_1 is discharged through V_{OL} :

$$V_{TLH} = V_{OL} + (V_{THL} - V_{OL})e^{-t_{discharge}/\tau}$$

Solving for t :

$$t_{discharge} = \tau \ln\left(\frac{V_{TLH} - V_{OL}}{V_{THL} - V_{OL}}\right)$$

Where:

$t_{discharge}$ = time for the capacitor to discharge from V_{THL} to V_{TLH} .

If $V_{OH} = V_{DD}$ and $V_{OL} = V_{SS}$, then $V_{THL} = 2/3 V_{DD}$ and $V_{TLH} = 1/3 V_{DD}$ as shown in the above example. Then t_{charge} and $t_{discharge}$ are as follows:

$$t_{charge} = 0.693 R_1 C_1$$

$$t_{discharge} = 0.693 R_1 C_1$$

Therefore, the oscillation frequency for this example is:

$$frequency = \frac{1}{1.386 R_1 C_1} = \frac{1}{t_{charge} + t_{discharge}}$$

Figure 16 shows the voltage waveforms of the oscillator inputs and output.

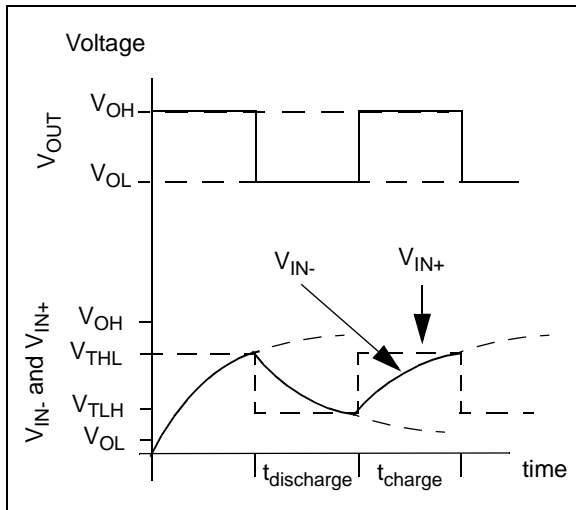


FIGURE 16: Graphical representation of the oscillator circuit voltage.

From this example, it can be shown that if R_2 , R_3 and R_4 have equal values, then the charge and discharge time will be the same. However, if the values of R_3 and R_4 change, then the oscillator duty cycle and frequency will change. A $\pm 1\%$ change in R_2 offsets the trip voltages with equal magnitude, but it does not affect the oscillation frequency.

APPENDIX C: ERROR ANALYSIS

Error analysis is useful when predicting the manufacturing variability, temperature stability and the drift in accuracy over time. An error analysis is not a replacement for development or verification tests. The oscillator's performance should always be verified by building and testing the circuit. An error analysis is a useful tool to estimate the accuracy of an oscillator and to provide a comparison on the performance of different circuits, such as the state variable and relaxation oscillator.

The first step in performing an error analysis is to calculate the shift of the oscillation frequency or sensitivity from factors such as tolerance, temperature coefficient and drift of the resistors and capacitors. Sensitivity is a measure of the change in the output (ΔY) per change in the input (ΔX). The sensitivity of the components are calculated from the oscillation equation, derived in **Appendix B: "Derivation of Oscillation Equations"**. A sensitivity of -1/2 means that a 1% increase in the component resistance or capacitance will decrease the oscillation frequency by 0.5%. The sensitivity equations for the state variable oscillator are listed below:

$$S_X^Y = \frac{\left(\frac{\Delta Y}{Y}\right)}{\left(\frac{\Delta X}{X}\right)} = \frac{d \ln(Y)}{d \ln(X)}$$

$$\omega_o = \left(\frac{R_4}{R_1 R_2 R_3 C_1 C_2}\right)^{1/2} \quad (\omega_o = 2\pi f)$$

$$S_{R_1}^{\omega_o} = S_{R_2}^{\omega_o} = S_{R_3}^{\omega_o} = -S_{R_4}^{\omega_o} = S_{C_1}^{\omega_o} = S_{C_2}^{\omega_o} = -1/2$$

An error analysis of the oscillator can be performed by either a Monte Carlo or a root-square-sum (RSS) analysis. The Monte Carlo analysis can be performed using a SPICE model or MathCad[®], a mathematical analysis program. The Monte Carlo analysis uses a statistical model of each circuit component and simulates the circuit's performance by randomly varying each component. A large number of simulated circuits can be easily evaluated and the variance of the frequency output can be analyzed.

The RSS error is easy to evaluate and will be used to predict and compare the expected performance of the state variable and relaxation oscillators. The RSS analysis consists of listing the magnitude of all the error terms and then multiplying the terms by the component sensitivity factor. Next, the sum of the square of each error is calculated. Finally, the RSS value is found by calculating the square root of the sum of the squared error terms. Listed below is the RSS error equation.

$$\text{Worst Case} = \sum_{k=1}^n \left| S_{\varepsilon_k}^O \varepsilon_k \right|$$

$$RSS = \sqrt{\sum_{k=1}^n (S_{\varepsilon_k}^O \varepsilon_k)^2}$$

Where:

$S_{\varepsilon_1}^O$ = sensitivity factor

ε_n = error terms

One limitation of the RSS method is that the error terms are usually determined using the worst-case specification or the maximum or minimum value listed on the component's data sheet. If worst-case specifications are used in the RSS analysis, the estimate of the error will usually be more pessimistic than the error measured with the hardware. Also, the RSS method assumes that the error terms are independent and can be modeled by a standard distribution curve.

The worst-case analysis consists of calculating the sum all of the error terms multiplied by the sensitivity weighting factor. This provides an estimation of the theoretical minimum or maximum value of the output. The insight given by worst-case analysis is limited because the probability that each component is at a value that maximizes the error is statistically unlikely, especially as the circuit component count increases.

APPENDIX D: ERROR ANALYSIS OF THE RELAXATION OSCILLATOR'S COMPARATOR

The non-ideal characteristics of a comparator, V_{OS} , I_B and output current limit and its effect over V_{OH} and V_{OL} were ignored for simplification, as shown in **Appendix B: "Derivation of Oscillation Equations"**. However, there will always be some voltage difference between the two inputs due to the mismatch in the comparator's input circuit. This voltage difference is specified in the data sheets as offset voltage (V_{OS}). The typical offset voltage for the MCP6541 is ± 1.5 mV, while the maximum limit is specified at ± 7 mV. In addition, the input bias current must also be analyzed. The high-impedance CMOS inputs of the comparator result in an I_B current of typically 1 pA at room temperature and about 100 pA over temperature.

The comparator offset voltage can be considered to be an additional voltage source that is added to the trip voltages. Therefore, the expected trip voltage maximum span becomes $V_{THL} \pm 1.5$ mV and $V_{TLH} \pm 1.5$ mV for the MCP6541. By substituting the effect of offset voltage over the trip voltages in the equation listed below, it can be shown that the typical offset voltage introduces a frequency oscillation ($f_{V_{OS}}$) error of less than 0.065%. The worst-case offset voltage of ± 7 mV introduces 0.3% tolerance over the frequency measurement, as shown below:

$$f_{V_{OS}} = \frac{I}{2\tau \ln\left(\frac{V_{THL} + V_{OS} - V_{OH}}{V_{TLH} + V_{OS} - V_{OH}}\right)}$$

Another error factor that could change the oscillation duty cycle and frequency is the effect of temperature over the op amp offset voltage and input bias current. However, the MCP6541 V_{OS} drift over temperature of ± 3 μ V/ $^{\circ}$ C (typ) is relatively small when compared to a typical V_{OS} of ± 1.5 mV. The shift of V_{OS} between $+25^{\circ}$ C and $+125^{\circ}$ C is equal to approximately ± 0.3 mV. Therefore, the effect of V_{OS} over temperature is negligible and the only dominating error source over temperature becomes the input bias current. The effect of input bias current can be calculated as shown in the following equations:

$$V_{THL} = \frac{I}{\left(\frac{I}{R_2} + \frac{I}{R_3} + \frac{I}{R_4}\right) \times \left(\frac{V_{DD}}{R_2} + \frac{V_{OH}}{R_3} + I_B\right)}$$

$$V_{TLH} = \frac{I}{\left(\frac{I}{R_2} + \frac{I}{R_3} + \frac{I}{R_4}\right) \times \left(\frac{V_{DD}}{R_2} + \frac{V_{OL}}{R_3} + I_B\right)}$$

Where:
 I_B = Input Bias Current

From these equations, it can be shown that the worst-case effect of I_B over the frequency measurement is 0.0002%. Therefore, the V_{OS} and the I_B current of the comparator have relatively minimal effect over the circuit accuracy.

A major limitation in the inaccuracy of the relaxation oscillator is the comparator's output current drive capability. The oscillation frequency depends on R_1 and C_1 . R_1 (RTD) is also used to limit the comparator sink and source current. If the output current is too high, the circuit may not work at start-up (when power is applied). It is recommended that the maximum sink or source current from the comparator be less than one-fifth (1/5) of the Output Short Circuit Current (I_{SC}). The MCP6541 has a I_{SC} specified as 50 mA (typ) for $V_{DD} = 5V$.

$$I_{OUT_MAX} = \frac{I_{SC}}{5} = \frac{50mA}{5} = 10mA$$

$$R_{1_MIN} = \frac{V_{DD}}{I_{OUT_MAX}} = \frac{5V}{10mA} = 500\Omega$$

Where:
 I_{OUT_MAX} = recommended maximum output current
 R_{1_MIN} = recommended minimum sensor resistance

According to the source current limit, R_1 should not be less than 500 Ω . The resistance of the RTD is equal to approximately 800 Ω at -50° C.

The magnitude of resistor R_1 also has an effect on the comparator output voltages V_{OH} and V_{OL} . The MCP6541 specifications of 200 mV headroom ($V_{DD} - V_{OH}$ and $V_{SS} + V_{OL}$) are specified at a source and sink current of ± 2 mA. If the output current level exceeds ± 2 mA, the output voltage limit decreases. This changes the expected trip voltages (V_{THL} and V_{TLH}). The change does not affect frequency, assuming the change in V_{OH} and V_{OL} are symmetrical, but the expected trip voltages will be shifted.

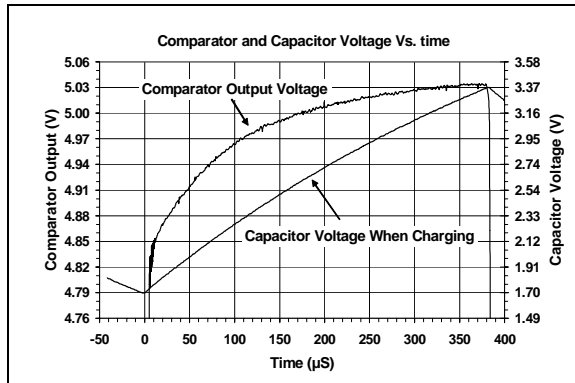


FIGURE 17: Effect of increasing source current from the comparator over V_{OH} at -51°C ($R_1 = 801\Omega$).

However, since V_{OH} and V_{OL} are voltages that charge and discharge the capacitor C_1 , any change in these voltages compromises the oscillation frequency. Figure 17 shows the effect of source current over the comparator output voltage headroom. It shows that when the capacitor begins to charge from V_{TLH} ($\approx 1.7\text{V}$) to V_{DD} , the required charging (source) current from the comparator increases. The increase in the source current compromises the comparator output voltage headroom, or V_{OH} decreases. The figure shows that during the first few microseconds, V_{OH} decreased by as much as 200 mV. The drop in the output voltage due to limited source current increases the expected time required to charge the capacitor (C_1). The increase in the time relative to an ideal oscillation output is approximately 6 μs , or 12 μs for the complete cycle. The output current limit introduces an error of approximately 1.5% in the frequency measurement, which correlates with the measured data shown in Table 5.

The frequency error due to the comparator source current and output voltage headroom limit can be minimized by reducing the charging current. This requires using a larger resistance RTD sensor and a smaller capacitor.

Two other comparator errors that must be considered are the propagation delay and output rise/fall time, which are limited by the comparator output slew rate. Propagation delay is defined as the time it takes for a 50% change at the input to make a 50% change at the output. The propagation delay of the MCP6541 is typically 4 μs . The comparator slew rate determines the time it takes for the output to reach the rails. The slew rate limitation is primarily caused by parasitic capacitance at the output of the comparator. For the MCP6541, the slew rate is measured to be 5V/ μs (typ). The error introduced due to the MCP6541 comparator's propagation delay and output slew rate is estimated to be approximately 1% for an oscillation frequency of 1000 Hz. The effect of the error due to propagation delay and slew rate over temperature is relatively small, when compared to the output current limit error.

AN895

NOTES:

Note the following details of the code protection feature on Microchip devices:

- Microchip products meet the specification contained in their particular Microchip Data Sheet.
- Microchip believes that its family of products is one of the most secure families of its kind on the market today, when used in the intended manner and under normal conditions.
- There are dishonest and possibly illegal methods used to breach the code protection feature. All of these methods, to our knowledge, require using the Microchip products in a manner outside the operating specifications contained in Microchip's Data Sheets. Most likely, the person doing so is engaged in theft of intellectual property.
- Microchip is willing to work with the customer who is concerned about the integrity of their code.
- Neither Microchip nor any other semiconductor manufacturer can guarantee the security of their code. Code protection does not mean that we are guaranteeing the product as "unbreakable."

Code protection is constantly evolving. We at Microchip are committed to continuously improving the code protection features of our products. Attempts to break Microchip's code protection feature may be a violation of the Digital Millennium Copyright Act. If such acts allow unauthorized access to your software or other copyrighted work, you may have a right to sue for relief under that Act.

Information contained in this publication regarding device applications and the like is intended through suggestion only and may be superseded by updates. It is your responsibility to ensure that your application meets with your specifications. No representation or warranty is given and no liability is assumed by Microchip Technology Incorporated with respect to the accuracy or use of such information, or infringement of patents or other intellectual property rights arising from such use or otherwise. Use of Microchip's products as critical components in life support systems is not authorized except with express written approval by Microchip. No licenses are conveyed, implicitly or otherwise, under any intellectual property rights.

Trademarks

The Microchip name and logo, the Microchip logo, Accuron, dsPIC, KEELoQ, MPLAB, PIC, PICmicro, PICSTART, PRO MATE, PowerSmart and rPIC are registered trademarks of Microchip Technology Incorporated in the U.S.A. and other countries.

AmpLab, FilterLab, microID, MXDEV, MXLAB, PICMASTER, SEEVAL, SmartShunt and The Embedded Control Solutions Company are registered trademarks of Microchip Technology Incorporated in the U.S.A.

Application Maestro, dsPICDEM, dsPICDEM.net, dsPICworks, ECAN, ECONOMONITOR, FanSense, FlexROM, fuzzyLAB, In-Circuit Serial Programming, ICSP, ICEPIC, Migratable Memory, MPASM, MPLIB, MPLINK, MPSIM, PICkit, PICDEM, PICDEM.net, PICtail, PowerCal, PowerInfo, PowerMate, PowerTool, rLAB, Select Mode, SmartSensor, SmartTel and Total Endurance are trademarks of Microchip Technology Incorporated in the U.S.A. and other countries.

SQTP is a service mark of Microchip Technology Incorporated in the U.S.A.

All other trademarks mentioned herein are property of their respective companies.

© 2004, Microchip Technology Incorporated, Printed in the U.S.A., All Rights Reserved.

 Printed on recycled paper.

**QUALITY MANAGEMENT SYSTEM
CERTIFIED BY DNV
== ISO/TS 16949:2002 ==**

Microchip received ISO/TS-16949:2002 quality system certification for its worldwide headquarters, design and wafer fabrication facilities in Chandler and Tempe, Arizona and Mountain View, California in October 2003. The Company's quality system processes and procedures are for its PICmicro® 8-bit MCUs, KEELoQ® code hopping devices, Serial EEPROMs, microperipherals, nonvolatile memory and analog products. In addition, Microchip's quality system for the design and manufacture of development systems is ISO 9001:2000 certified.



WORLDWIDE SALES AND SERVICE

AMERICAS

Corporate Office

2355 West Chandler Blvd.
Chandler, AZ 85224-6199
Tel: 480-792-7200
Fax: 480-792-7277
Technical Support: 480-792-7627
Web Address: <http://www.microchip.com>

Atlanta

3780 Mansell Road, Suite 130
Alpharetta, GA 30022
Tel: 770-640-0034
Fax: 770-640-0307

Boston

2 Lan Drive, Suite 120
Westford, MA 01886
Tel: 978-692-3848
Fax: 978-692-3821

Chicago

333 Pierce Road, Suite 180
Itasca, IL 60143
Tel: 630-285-0071
Fax: 630-285-0075

Dallas

4570 Westgrove Drive, Suite 160
Addison, TX 75001
Tel: 972-818-7423
Fax: 972-818-2924

Detroit

Tri-Atria Office Building
32255 Northwestern Highway, Suite 190
Farmington Hills, MI 48334
Tel: 248-538-2250
Fax: 248-538-2260

Kokomo

2767 S. Albright Road
Kokomo, IN 46902
Tel: 765-864-8360
Fax: 765-864-8387

Los Angeles

18201 Von Karman, Suite 1090
Irvine, CA 92612
Tel: 949-263-1888
Fax: 949-263-1338

San Jose

1300 Terra Bella Avenue
Mountain View, CA 94043
Tel: 650-215-1444
Fax: 650-961-0286

Toronto

6285 Northam Drive, Suite 108
Mississauga, Ontario L4V 1X5, Canada
Tel: 905-673-0699
Fax: 905-673-6509

ASIA/PACIFIC

Australia

Suite 22, 41 Rawson Street
Epping 2121, NSW
Australia
Tel: 61-2-9868-6733
Fax: 61-2-9868-6755

China - Beijing

Unit 706B
Wan Tai Bei Hai Bldg.
No. 6 Chaoyangmen Bei Str.
Beijing, 100027, China
Tel: 86-10-85282100
Fax: 86-10-85282104

China - Chengdu

Rm. 2401-2402, 24th Floor,
Ming Xing Financial Tower
No. 88 TIDU Street
Chengdu 610016, China
Tel: 86-28-86766200
Fax: 86-28-86766599

China - Fuzhou

Unit 28F, World Trade Plaza
No. 71 Wusi Road
Fuzhou 350001, China
Tel: 86-591-7503506
Fax: 86-591-7503521

China - Hong Kong SAR

Unit 901-6, Tower 2, Metroplaza
223 Hing Fong Road
Kwai Fong, N.T., Hong Kong
Tel: 852-2401-1200
Fax: 852-2401-3431

China - Shanghai

Room 701, Bldg. B
Far East International Plaza
No. 317 Xian Xia Road
Shanghai, 200051
Tel: 86-21-6275-5700
Fax: 86-21-6275-5060

China - Shenzhen

Rm. 1812, 18/F, Building A, United Plaza
No. 5022 Binhe Road, Futian District
Shenzhen 518033, China
Tel: 86-755-82901380
Fax: 86-755-8295-1393

China - Shunde

Room 401, Hongjian Building, No. 2
Fengxiangnan Road, Ronggui Town, Shunde
District, Foshan City, Guangdong 528303, China
Tel: 86-757-28395507 Fax: 86-757-28395571

China - Qingdao

Rm. B505A, Fullhope Plaza,
No. 12 Hong Kong Central Rd.
Qingdao 266071, China
Tel: 86-532-5027355 Fax: 86-532-5027205

India

Divyasree Chambers
1 Floor, Wing A (A3/A4)
No. 11, O'Shaughnessy Road
Bangalore, 560 025, India
Tel: 91-80-22290061 Fax: 91-80-22290062

Japan

Benex S-1 6F
3-18-20, Shinyokohama
Kohoku-Ku, Yokohama-shi
Kanagawa, 222-0033, Japan
Tel: 81-45-471- 6166 Fax: 81-45-471-6122

Korea

168-1, Youngbo Bldg. 3 Floor
Samsung-Dong, Kangnam-Ku
Seoul, Korea 135-882
Tel: 82-2-554-7200 Fax: 82-2-558-5932 or
82-2-558-5934

Singapore

200 Middle Road
#07-02 Prime Centre
Singapore, 188980
Tel: 65-6334-8870 Fax: 65-6334-8850

Taiwan

Kaohsiung Branch
30F - 1 No. 8
Min Chuan 2nd Road
Kaohsiung 806, Taiwan
Tel: 886-7-536-4818
Fax: 886-7-536-4803

Taiwan

Taiwan Branch
11F-3, No. 207
Tung Hua North Road
Taipei, 105, Taiwan
Tel: 886-2-2717-7175 Fax: 886-2-2545-0139

EUROPE

Austria

Durisolstrasse 2
A-4600 Wels
Austria
Tel: 43-7242-2244-399
Fax: 43-7242-2244-393

Denmark

Regus Business Centre
Lautrup høj 1-3
Ballerup DK-2750 Denmark
Tel: 45-4420-9895 Fax: 45-4420-9910

France

Parc d'Activite du Moulin de Massy
43 Rue du Saule Trapu
Batiment A - Ier Etage
91300 Massy, France
Tel: 33-1-69-53-63-20
Fax: 33-1-69-30-90-79

Germany

Steinheilstrasse 10
D-85737 Ismaning, Germany
Tel: 49-89-627-144-0
Fax: 49-89-627-144-44

Italy

Via Quasimodo, 12
20025 Legnano (MI)
Milan, Italy
Tel: 39-0331-742611
Fax: 39-0331-466781

Netherlands

P. A. De Biesbosch 14
NL-5152 SC Drunen, Netherlands
Tel: 31-416-690399
Fax: 31-416-690340

United Kingdom

505 Eskdale Road
Winnersh Triangle
Wokingham
Berkshire, England RG41 5TU
Tel: 44-118-921-5869
Fax: 44-118-921-5820

02/17/04